nature chemistry

SUPPLEMENTARY INFORMATION

DOI: 10.1038/NCHEM.1627

Probing the biophysical interplay between a viral genome and its capsid

Authors:

J. Snijder, C. Uetrecht, R.J. Rose, R. Sanchez-Eugenia, G.A. Marti, J. Agirre, D.M.A. Guérin, G.J.L. Wuite, A.J.R. Heck, W.H. Roos

Index

Supplementary Methods:

Autofluorescence

We performed tryptophan fluorescence measurements by exciting at 295nm and recording between 305 and 420nm in a FluoroMax fluorimeter (Horiba Jobin-Yvon). TrV samples were at 0.1mg/mL at the indicated pH.

Native-PAGE

Native polyacrylamide gels prepared at 5% were run with no sample loaded for 30 minutes at 140V and 4ºC in order to equilibrate them with the running buffer (2.5mM Tris-HCl pH 8.2 and 19mM glycine). 20µL of TrV samples at 0.1mg/mL were mixed with 5µL of native loading buffer (0.25M Tris-HCl pH6.8, 50% glycerol, 60mM EDTA and 0.0125% (w/v) bromophenol blue). Loaded samples and molecular weight markers (High Molecular Weight Kit, GE Healthcare) were run for 4 hours at 100V and 4ºC. Finally gels were stained with staining solution (50% methanol, 10% acetic acid and 0.25% w/v R-250 Coomassie Blue) for 20 minutes and unstained overnight with 10% acetic acid solution.

Computed electrostatic binding energies

Adaptive Poisson-Boltzmann Solver (APBS) software was used to calculate the binding energy between VP1/2/3 protomers within and between pentons. The binding free energy between protomer A and the rest of the complex B (either the other 4 penton protomers or the adjacent penton) was calculated taking into account the unfavorable process of desolvation of both proteins and the likely favorable process of electrostatic interaction between them: $\Delta G_{binding} = \Delta G_{desolA} + \Delta G_{desolB} + E_{elec.AB}$. The desolvation energies of protomers correspond to the loss of electrostatic interaction energy between the solvent and the protomer upon binding, and was calculated for each protomer by first calculating the electrostatic energy of the complex A-B with B protomer charges set to 0 (E_1) and calculating the electrostatic energy of A (E_2). Then, the desolvation energy of protomer A was obtained by: $\Delta G_{desol\ A} = E_1 - E_2$. Finally, the electrostatic energy was calculated as the electrostatic potential generated by protomer A at the position of atomic charges of protomer B:

$$E_{electrostaticA-B} = \sum_{i}^{N} \varphi_i \cdot q_i$$

Electrostatic interaction energy between two molecules, A and B.

APBS input settings were: *i)* Linearized Poisson-Boltzmann equation was solved. *ii)* The number of grid points was 321 x 353 x 417, the length of the coarse grid was 214.977 x 262.910 x 312.543 and of the fine grid 146.457 x 174.653 x 203.849. *iii)* Protein dielectric constant was set to 2 and the solvent dielectric constant was set to 78.54. *iv)* Dissolvated ions were taken into account as follows: ion charge +1 at a concentration of 0.150M with a radius of 2.0Å and ion charge -1 at a concentration of 0.150M with the same radius.

Genome Packing Density

The packing density of the genomes in TrV and phage λ were calculated by dividing the total number of nucleotides by the inner volume of the capsid. Capsids were approximated as spheres to calculate the inner volumes. TrV was taken to have an inner radius of 11.7 nm, giving an inner volume of 6709 nm^3. The radius of phage λ was taken as 28.2 nm, giving an inner volume of 93937 nm^3. The total number of nucleotides was taken as 9010 for TrV and as 2*48502 for phage λ.

Supplementary data

Tab. S1. Experimental vs. sequence derived masses of TrV. The stated errors are the standard deviations of masses derived from different charge states within one spectrum, except in the case of "r-empty", which is the standard deviation over five replicate analyses.

complex	mass_avg (kDa)	mass_stdev (kDa)	Theoretical (kDa)	
			sequence[a]	exp[b]
penton	444.8	0.3	446.1	446.5
decamer	888.4	0.3	892.1	893.1
r-empty capsid	5362	2.5	5353	5359
virion	No resolved charge states		8252	8258
VP1	29.774	0.004	29.719	
VP2	28.405	0.0009	28.401	
VP3	31.129	0.0009	31.093	
VP4	5.504	0.0002	5.503	

[a]based on sequence, verified by genomic sequencing and LC-MS/MS
[b]based on experimental VP monomer masses

Tab. S2. Cross sections of TrV disassembly products measured by IMS. Stated errors are standard deviations over triplicate experiments.

			Experimental[a]		Theoretical	
complex	origin		Ω (nm^2)	stdev	from PDB code: 3NAP[b]	as globular[c]
penton	pH		169	3	158	138
	urea	low charges	165	1		
		high charges	170	0.2		
			183	9		
			203	16		
penton-dimer	urea		250	3	282	225

[a]Average over all charge states and triplicate analysis
[b]From projection approximation (PA) calculations, note that residues are missing from the pdb coordinates, resulting in underestimation of the cross section
[c]The expected cross section of a globular protein as estimated with the experimentally obtained fit of globular proteins presented in the main text.

Tab. S3. Particle diameters as determined by AFM. Heights were corrected by the estimated indentation during imaging, typically well below 1 nm. Stated errors are Standard Error of the Mean (SEM).

		corrected particle height (nm)		
particle type	**pH**	**avg**	**SEM**	**n**
n-empty	6.8	34.0	0.2	32
	8	33.7	0.2	36
	9	33.6	0.3	27
r-empty	6.8	34.3	0.2	14
	9	34.3	0.3	29
virion	6.8	34.1	0.2	25
	8	34.0	0.2	8

Tab. S4. Penton dimensions as determined from AFM imaging. The 'ppd' denotes the peak-to-peak distance: the lateral separation between adjacent five-fold related subunits as can be distinguished in the AFM image. Stated errors are Standard Error of the Mean (SEM). The height of the penton in the crystal structure of TrV (PDB code: 3NAP) is approximately 7 nm and adjacent VP1 protrusions are separated by approximately 6 nm.

	height (nm)			ppd (nm)		
type	**avg**	**SEM**	**n**	**avg**	**SEM**	**n**
force-induced	6.7	0.03	143	6.3	0.1	69
pH-induced	6.6	0.05	58	6.5	0.08	77

Tab. S5. Mechanical properties of TrV particles determined by AFM nanoindentation. For virion particles, the indicated subclassification into intact virion, uncoating intermediate and r-empty capsid was based on the density plot presented in the main text. 'r-empty' was defined as all particles with F_{break} < 2 nN, 'uncoating intermediate' as F_{break} > 2 nN and k < 1 N/m, all remaining particles were classified as 'intact virion'. Stated errors are Standard Error of the Mean (SEM).

			k (N/m)			F_{break} (nN)		
		pH	**avg**	**SEM**	**n**	**avg**	**SEM**	**n**
virion	**intact virion**	7	1.47	0.06	34	3.62	0.15	34
		8	1.34	0.14	6	3.81	0.17	6
		8->7	1.47	0.06	19	3.80	0.08	19
		combined	**1.46**	**0.04**	**59**	**3.69**	**0.09**	**59**
	uncoating intermediate	7	0.63	0.08	12	3.15	0.26	12
		8	0.49	0.07	12	3.24	0.16	12
		8->7	0.67	0.08	7	3.04	0.19	7
		combined	**0.58**	**0.05**	**31**	**3.16**	**0.12**	**31**
	r-empty	7	0.50	0.09	11	0.86	0.09	16
		8	0.42	0.12	14	0.77	0.11	14
		9	0.37	0.07	27	0.92	0.06	29
		8->7	0.46	0.12	8	1.35	0.25	8
		9->7	0.46	0.05	14	0.87	0.07	14
		combined	**0.43**	**0.04**	**74**	**0.92**	**0.05**	**81**
n-empty		7	0.52	0.07	27	0.81	0.04	32
		8	0.52	0.05	31	0.91	0.06	35
		9	0.37	0.05	26	0.90	0.06	26
		combined	**0.47**	**0.03**	**84**	**0.87**	**0.03**	**93**

Tab. S6. Particle diameters as determined by Ion Mobility Spectrometry. There is no significant difference (> 2 Standard Deviation, SD) between empty capsids and the virion.

	diameter (nm)	
particle type	**avg**	**SD**
n-empty	33.3	1.5
r-empty	34	2
virion	36.5	0.4

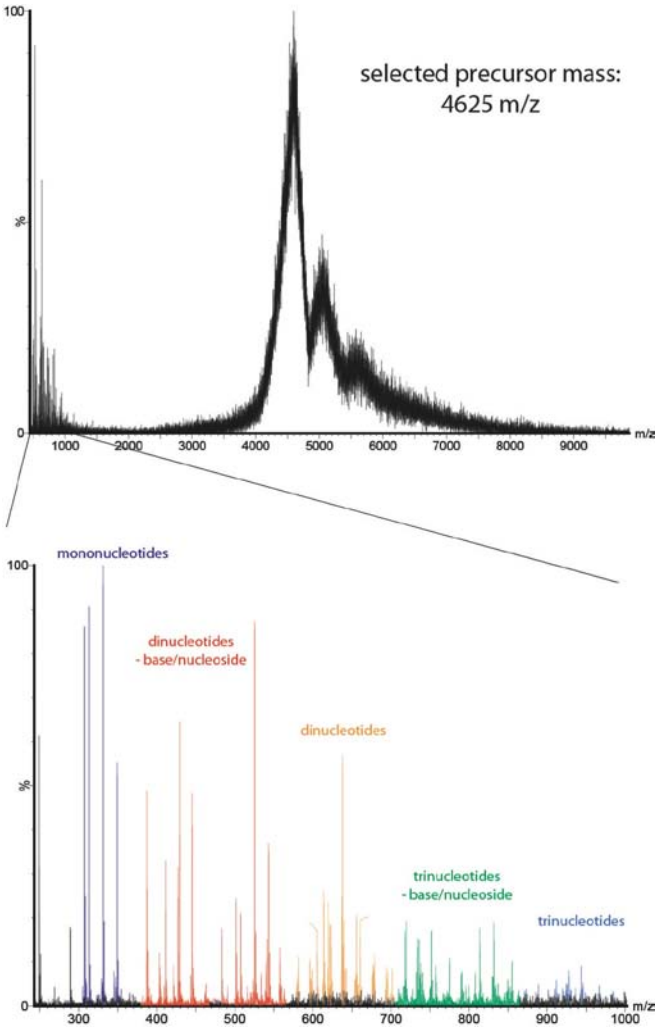

Fig. S1. Tandem MS of unresolved baseline signal in the virion at pH >8. Top: tandem MS of 4625 *m/z* precursor ions, showing both extensive fragmentation and neutral loss. Bottom: zoom-in of ribonucleotide fragments of the 4625 *m/z* precursor ions.

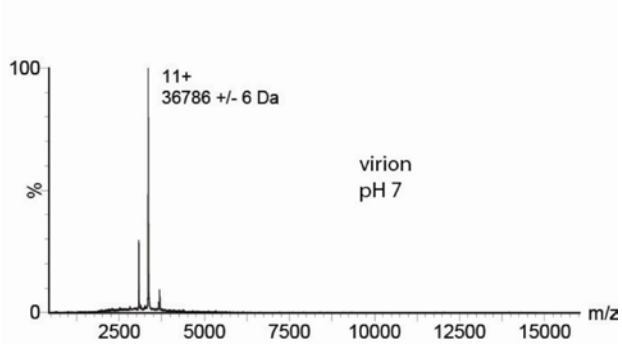

Fig. S2. Low *m/z* region of the virion at neutral pH. There is no signal for ssRNA, VP4 and pentons. There is a distinguishable charge state distribution for this unknown 36 kDa component referred to in the main text, showing that it is unrelated to alkaline-trigged uncoating.

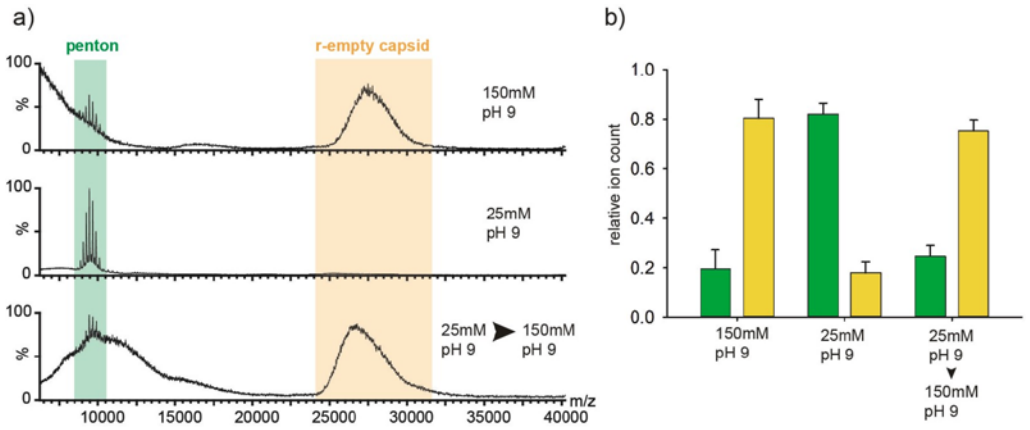

Fig. S3. Pentons generated from the virion under alkaline conditions are assembly competent. a) Mass spectra of virion samples incubated for one day at 150mM pH 9 or 25mM pH 9 and after one day 25mM, one day 150mM pH 9. Both r-empty capsids and penton are observed at 150mM ionic strength. More penton is formed under low ionic strength conditions. When the 25mM pH 9 sample is subsequently transferred to 150mM and incubated for one additional day, more r-empty capsid is formed. Hence, pentons can reassemble into empty capsids. b) Average relative ion count for penton (green) and capsid (yellow) from duplicate experiments. Error bars are SD.

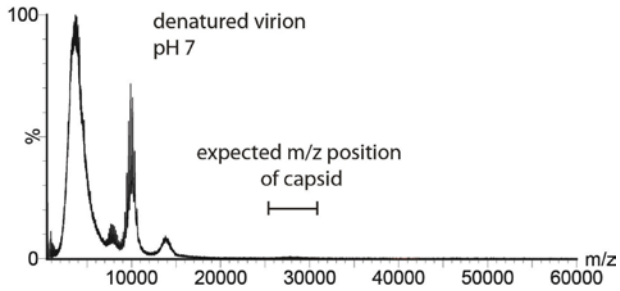

Fig. S4. Overview scan of a urea denatured virion sample. There is no substantial signal for the empty capsid, showing that reassembly does not occur with denatured pentons/decamers.

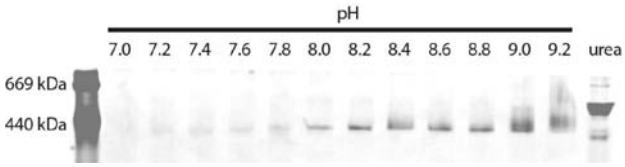

Fig S5. Native gel of virion at increasing pH and after urea denaturation. There is an increasing amount of ~440 kDa product on gel with increasing pH. This is consistent with the appearance of pentons, confirming that alkaline-triggered uncoating occurs via disassembly of the capsid.

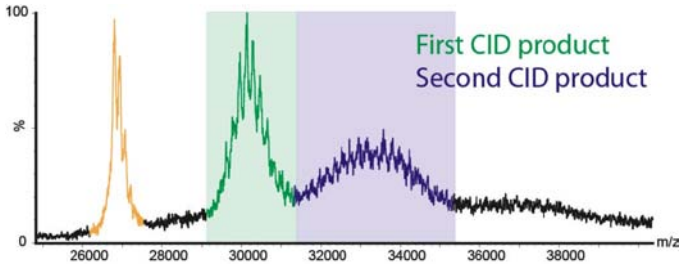

Fig S6. Tandem MS of r-empty capsids confirms the mass assignment, thus confirming release of ssRNA and VP4. Ions of the r-empty capsid (yellow) are selected in the instrument and subjected to high collision voltage (260V with xenon as collision gas). This results in sequential dissociation of VP subunits. The large product ions indicated in green and blue correspond to the loss of one and two VP subunits, respectively. Their respective masses are calculated at 5332 ± 2 and 5306 ± 1 kDa, corresponding to the loss of first 29.5 and then another 26.5 kDa (stated errors are SD). This matches the expected masses of VP2/3 to within the error margin, confirming that the precursor is 60*VP1/2/3 without any discernible inclusion of ssRNA or VP4.

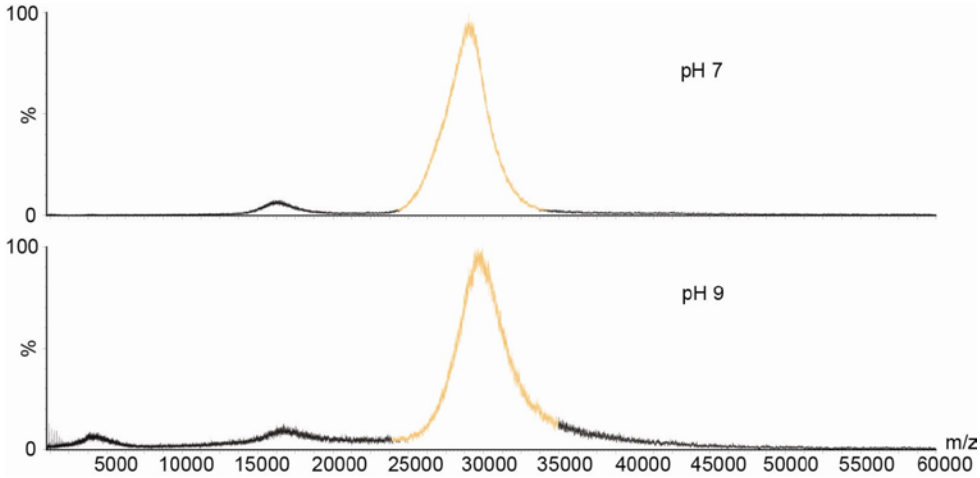

Fig. S7. Native MS of n-empty capsids. There are no distinguishable disassembly products at alkaline pH and there is no notable shift in peak-position of the n-empty capsid under alkaline pH. This shows that there is no conformational change to the effect of a larger chargeable surface area under alkaline conditions. Also, it supports the data demonstrating that virion disassembly at alkaline pH is triggered by the ssRNA.

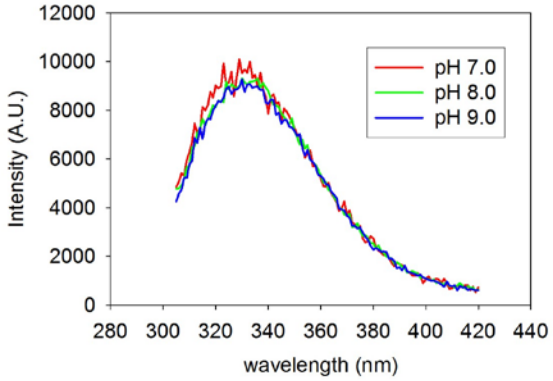

Fig. S8. Auto-fluorescence of TrV virions at increasing pH. There is only a marginal pH-induced change in the auto-fluorescence spectra of TrV that likely relates to deprotonation of tyrosine residues. Therefore, there are no major conformational changes in the vicinity of aromatic residues. Note that TrV contains in total five tryptophan residues, none of which is exposed in either the full capsid or free penton (PDB code: 3NAP).

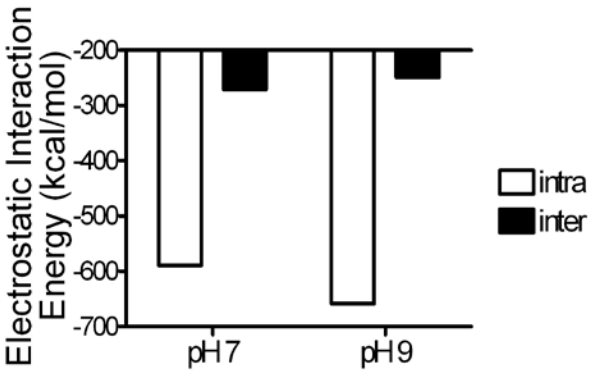

Fig. S9. APBS calculations of the electrostatic interaction potential of VP1/2/3 protomers within (intra) and between (inter) pentons (see methods). The interaction is stronger within pentons than between pentons. There is no substantial difference between pH 7 and pH 9. This explains the occurrence of pentons as disassembly products and supports the hypothesis that the ssRNA genome triggers alkaline-induced disassembly in the virion.

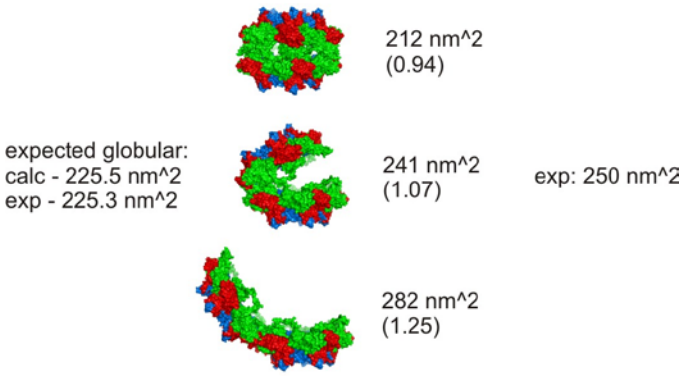

Fig. S10. Assembly incompetent penton-dimers hinge on the penton-penton interface. Collision cross section calculations of the penton-dimers. 'Expected globular' refers to the expected cross section when entering the molecular weight of the assembly into the obtained fit of all globular assemblies. 'calc' denotes the expected cross section from the observed trend of MobCal PA calculations of globular proteins, 'exp' denotes the expected cross section from the observed experimental trend. The structures represent a penton-dimers model with an increasing angle between pentons. The bottom structure represents the angle as observed in the complete capsid of TrV (PDB code: 3NAP). The values correspond to the PA cross section of that model, the values in parentheses are the relative cross section compared to 'expected globular'. These calculations suggest that the pentons hinge on their interface, thus explaining the relatively low cross section of the penton-dimers compared to the pentons.

Fig. S11. AFM imaging of alkaline-triggered disassembly products. This shows that pentons are present in the virion sample at pH 9. Left image is 100x100 nm in xy and approximately 10 nm in z.

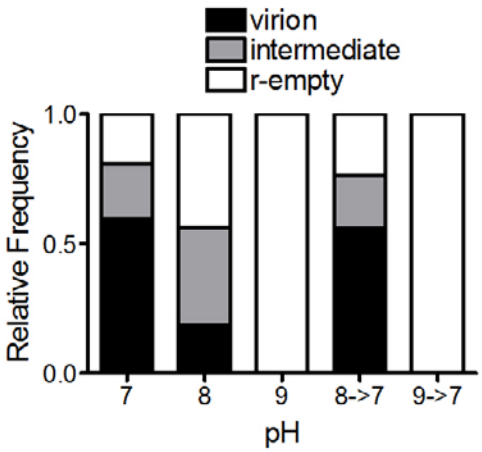

Fig. S12. AFM data with the relative frequencies of virion, pre-disassemble state and r-empty capsid and reversibility of the transitions. There is a 2-fold increase of the uncoating intermediate (pre-disassemble state) at pH 8, and the transition is reversible. Reversing the pH from 9 to 7 does not result in reassembly of the virion (encapsidation of the ssRNA). Note that the increased frequency of the r-empty capsid at pH 8 is related to the time-scale. Samples at pH 8 are stored for several days over the course of the analysis, in the experiment of pH8 -> 7, the sample is incubated overnight before reversing the pH back to 7.

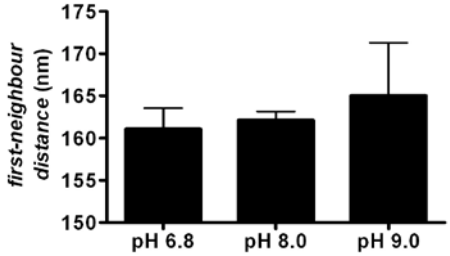

Fig. S13. Particle density in AFM imaging as a function of pH. The particle density was determined from several scans of 2x2 μm as the average first-neighbour distance. The particle density is constant over the tested pH range, confirming that the observed reassembly of virions into empty capsids does not arise from a sampling error.

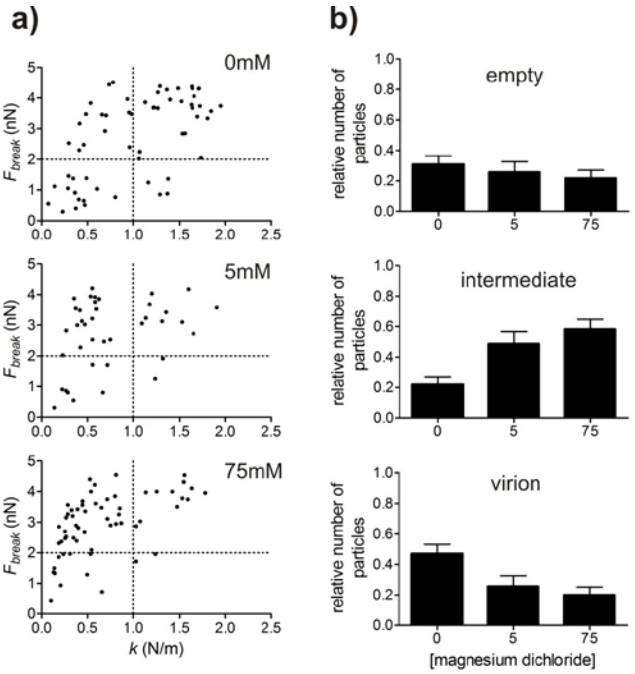

Fig. S14. AFM nanoindentation of TrV in the presence/absence of magnesium dichloride at pH 6.8. a) 2D-plots of spring constant *vs.* breaking force of TrV virion samples without magnesium dichloride and with 5 or 75mM magnesium dichloride. The boundaries used to classify different types of particles are indicated by dashed line and are the same as in the alkaline-triggered uncoating experiment: empty (F_{break} < 2 nN), 'intermediate' (F_{break} > 2 nN and k < 1 N/m) and virion (F_{break} > 2 nN and k > 1 N/m). b) Relative number of particles per particle-type, as a function of magnesium dichloride concentration. The error bars represent the relative SD as estimated assuming binomial distributions for each particle type (*e.g.* either 'empty' or 'not empty'): the errors were calculated as ((Npq)^0.5)/N, where N is the total number of particles, p is the relative frequency of a particular particle-type and $q = 1 - p$. Adding magnesium dichloride results in a shift to lower spring constant for ssRNA-filled particles, as apparent from the increased frequency of 'intermediates'. We also performed a control experiment with r-empty capsids to test the effect of 75mM magnesium dichloride on the mechanical response of the capsid alone at pH 6.8 and found no significant difference in spring constant or breaking force compared to the r-empty capsid without magnesium dichloride (k = 0.48 ± 0.06 N/m, F_{break} = 0.67 ± 0.03 nN, n = 16). This shows that the magnesium dichloride does not affect the protein-protein interactions, instead it must act on the ss-RNA.